

# Increased plasma cholesterol esterification by LCAT reduces diet-induced atherosclerosis in SR-BI knockout mice<sup>§</sup>

Seth G. Thacker,<sup>1,\*</sup> Xavier Rousset,<sup>1,\*</sup> Safiya Esmail,<sup>\*</sup> Abdalrahman Zarzour,<sup>\*</sup> Xueting Jin,<sup>†</sup> Heidi L. Collins,<sup>§</sup> Maureen Sampson,<sup>\*\*</sup> John Stonik,<sup>\*</sup> Stephen Demosky,<sup>\*</sup> Daniela A. Malide,<sup>††</sup> Lita Freeman,<sup>\*</sup> Boris L. Vaisman,<sup>\*</sup> Howard S. Kruth,<sup>†</sup> Steven J. Adelman,<sup>§</sup> and Alan T. Remaley<sup>2,\*</sup>

Lipoprotein Metabolism Section, Cardiovascular-Pulmonary Branch,<sup>\*</sup> Experimental Atherosclerosis Section, Center for Molecular,<sup>†</sup> and Light Microscopy Core,<sup>††</sup> National Heart, Lung, and Blood Institute, National Institutes of Health, Bethesda, MD 20892; Vascular Strategies LLC,<sup>§</sup> Plymouth Meeting, PA 19462; and Department of Laboratory Medicine,<sup>\*\*</sup> Clinical Center, National Institutes of Health, Bethesda, MD 20892

**Abstract** LCAT, a plasma enzyme that esterifies cholesterol, has been proposed to play an antiatherogenic role, but animal and epidemiologic studies have yielded conflicting results. To gain insight into LCAT and the role of free cholesterol (FC) in atherosclerosis, we examined the effect of LCAT over- and underexpression in diet-induced atherosclerosis in scavenger receptor class B member I-deficient [*Scarab*( $-/-$ )] mice, which have a secondary defect in cholesterol esterification. *Scarab*( $-/-$ ) $\times$ LCAT-null [*Lcat*( $-/-$ )] mice had a decrease in HDL-cholesterol and a high plasma ratio of FC/total cholesterol (TC) ( $0.88 \pm 0.033$ ) and a marked increase in VLDL-cholesterol (VLDL-C) on a high-fat diet. *Scarab*( $-/-$ ) $\times$ LCAT-transgenic (Tg) mice had lower levels of VLDL-C and a normal plasma FC/TC ratio ( $0.28 \pm 0.005$ ). Plasma from *Scarab*( $-/-$ ) $\times$ LCAT-Tg mice also showed an increase in cholesterol esterification during in vitro cholesterol efflux, but increased esterification did not appear to affect the overall rate of cholesterol efflux or hepatic uptake of cholesterol. *Scarab*( $-/-$ ) $\times$ LCAT-Tg mice also displayed a 51% decrease in aortic sinus atherosclerosis compared with *Scarab*( $-/-$ ) mice ( $P < 0.05$ ). **In summary, we demonstrate that increased cholesterol esterification by LCAT is atheroprotective, most likely through its ability to increase HDL levels and decrease pro-atherogenic apoB-containing lipoprotein particles.**—Thacker, S. G., X. Rousset, S. Esmail, A. Zarzour, X. Jin, H. L. Collins, M. Sampson, J. Stonik, S. Demosky, D. A. Malide, L. Freeman, B. L. Vaisman, H. S. Kruth, S. J. Adelman, and A. T. Remaley. **Increased plasma cholesterol esterification by LCAT reduces diet-induced atherosclerosis in SR-BI knockout mice.** *J. Lipid Res.* 2015. 56: 1282–1295.

**Supplementary key words** lecithin:cholesterol acyltransferase • scavenger receptor class B member I • knockout

This research was supported by intramural National Heart, Lung, and Blood Institute, National Institutes of Health funds.

Manuscript received 27 February 2014 and in revised form 27 April 2015.

Published, JLR Papers in Press, May 11, 2015  
DOI 10.1194/jlr.M048629

The reverse cholesterol transport (RCT) pathway plays a key role in protecting against atherosclerosis. During RCT, excess cholesterol is effluxed from peripheral cells, such as aortic macrophages, and is transported back to the liver where it can be excreted or converted to a bile salt. LCAT plays a vital role in this process (1), as it is the only known plasma enzyme that esterifies free cholesterol (FC). The esterification of cholesterol promotes net cholesterol efflux by trapping it in the hydrophobic core of lipoproteins, thus preventing its back exchange (2). Cholesterol esterification also promotes cholesterol efflux by increasing the concentration gradient of FC between cells and extracellular lipoprotein acceptors (2, 3). Radiolabeled cholesterol tracer studies in humans indicate that once esterified by LCAT, cholesteryl esters are preferentially returned to the liver (2), in part by scavenger receptor class B member I (SR-BI) (4, 5). As a consequence of its proposed anti-atherogenic effects, LCAT is now being investigated as a possible therapeutic target (6–9).

In addition to promoting RCT, the esterification of cholesterol may have other benefits in preventing the development of atherosclerosis. Excess FC in plasma membranes can adversely affect the function of numerous plasma membrane proteins, and high levels of FC are cytotoxic (10, 11). Inhibition of the intracellular esterification of

Abbreviations: FC, free cholesterol; FPLC, fast-protein LC; HDL-C, HDL-cholesterol; *Lcat*( $-/-$ ), LCAT-null; RBC, red blood cell; RCT, reverse cholesterol transport; *Scarab*( $-/-$ ), scavenger receptor class B member I-deficient;  $S^-L^+$ , *Scarab*( $-/-$ ) $\times$ *Lcat*( $+/+$ );  $S^-L^-$ , *Scarab*( $-/-$ ) $\times$ *Lcat*( $-/-$ );  $S^-L^{++}$ , *Scarab*( $-/-$ ) $\times$ LCAT-Tg; SR-BI, scavenger receptor class B member I; TC, total cholesterol; Tg, transgenic; VLDL-C, VLDL-cholesterol.

<sup>1</sup>S. G. Thacker and X. Rousset contributed equally to this work.

<sup>2</sup>To whom correspondence should be addressed.

e-mail: aremaley1@cc.nih.gov

<sup>§</sup>The online version of this article (available at <http://www.jlr.org>) contains supplementary data in the form of two figures, two tables, and text.

cholesterol by ACAT inhibitors has been shown to accelerate atherosclerosis and increase cardiovascular events in clinical trials (12). Recently, the enrichment of FC in red blood cell (RBC) plasma membranes has also been implicated in the development of atherosclerosis (13–15), and RBC cholesterol content has been proposed as a possible cardiovascular biomarker (15, 16). Patients with a wide variety of primary dyslipidemias, such as abetalipoproteinemia, for example, are known to have elevated levels of FC in RBC membranes due to an altered exchange of excess FC on lipoproteins with circulating RBCs (2, 17). The enrichment of FC in RBC membranes can lead to altered cell shape and function (18, 19). FC on lipoproteins is also known to exchange with the plasma membrane of platelets, and cholesterol enrichment has been demonstrated to promote platelet activation (20–22).

To better understand the role of LCAT, particularly in the context of increased FC, we describe here the development of two novel transgenic (Tg) mice, namely SR-BI-deficient [*Scarab*(-/-)] $\times$ LCAT-null [*Lcat*(-/-)] mice ( $S^{-}L^{-}$ ), which lack LCAT, and *Scarab*(-/-) $\times$ LCAT-Tg mice ( $S^{-}L^{+}$ ), which overexpress human LCAT. RBCs and platelets from *Scarab*(-/-) $\times$ *Lcat*(+/+) ( $S^{-}L^{+}$ ) mice are known to have elevated levels of FC (19), and HDL from these mice is increased in size and displays an impairment in cholesterol esterification, as only 40–50% of the cholesterol is esterified compared with approximately 75% observed in WT mice (23–28). The decrease in cholesterol esterification in  $S^{-}L^{+}$  mice is presumably because of the decreased efficiency of large HDL particles to activate LCAT (29, 30). Additionally,  $S^{-}L^{+}$  mice have been described as having an increased propensity to diet-induced atherosclerosis despite their increased HDL-cholesterol (HDL-C) levels, possibly because of decreased hepatic delivery of cholesterol (23–28).

In this study, we show that the alteration of LCAT expression in *Scarab*(-/-) mice results in profound changes in the percentage of cholesterol esterified and in the distribution of cholesterol on lipoproteins, RBCs, and platelets. Furthermore, we demonstrate that decreased cholesterol esterification caused by the loss of LCAT in  $S^{-}L^{-}$  mice further accentuates the development of atherosclerosis when compared with  $S^{-}L^{+}$  mice.

## MATERIALS AND METHODS

### Animal procedures

LCAT-Tg mice, containing 240 copies of the human LCAT gene, but with only a 2-fold increase in the rate of plasma cholesterol esterification (31), and *Lcat*(-/-) mice (32), both on a C57BL/6N background, were crossed with  $S^{-}L^{+}$  mice (Jackson Laboratory, stock number 3379) which were backcrossed three times onto the C57BL/6N background. The resultant new strains were designated as either  $S^{-}L^{++}$  or  $S^{-}L^{-}$  mice (31, 32). Probucol was added to the chow of  $S^{-}L^{+}$  mice to facilitate breeding (33). C57BL/6N mice (WT) were purchased from Taconic (Albany, NY). Mice were housed under controlled conditions, with a 12/12 h light/dark cycle, and fed either a standard rodent autoclaved

chow diet containing 4.0% fat (NIH31 chow diet; Zeigler Brothers Inc., Gardners, PA) or a Western diet (TD.88137 Adjusted Calories Diet; Harlan Teklad, Madison, WI). Only female mice were used in this study and, starting at 2 months of age, were fed ad libitum with a Western diet or chow diet for 7 months. All animal procedures were approved by a National Institutes of Health Institutional Animal Care and Use Committee (protocol H-0050R2).

### Plasma lipid and lipoprotein analysis

Unless otherwise noted, all chemicals used were obtained from Sigma-Aldrich (St. Louis, MO). Blood samples were collected from the periorbital sinus of eyes, with a heparinized capillary tube, and EDTA-plasma was obtained by centrifugation for 10 min at 3,000 g at 4°C. EDTA-whole blood (500  $\mu$ l) was used to determine blood cell populations, using a Cell-Dyn 3700 (Abbott, Abbott Park, IL). For lipid extraction, blood cells were washed with normal saline and centrifuged at 4°C, 3,000 g for 10 min. Lipids were extracted by lysing the RBCs with an equal volume of distilled water followed by extraction of lipids by an overnight incubation with 20 vol of chloroform/methanol (2:1). Total cholesterol (TC), FC, and phospholipids were analyzed by enzymatic assays from Wako Chemicals (Richmond, VA). Triglyceride levels were measured by an enzymatic assay from Roche Diagnostics (Indianapolis, IN). Lipoprotein profiles in plasma were obtained by fast-protein LC (FPLC) (Akta FPLC; GE Healthcare) on two Superose-6 columns in series. For each group, 400  $\mu$ l of pooled plasma from at least four mice was used for FPLC and lipids were measured enzymatically.

To analyze the protein content of FPLC fractions, 50  $\mu$ l from four fractions corresponding to 2 ml of elution volume were pooled together and 2 mg of lipid removal agent (Sigma) were added to concentrate lipoprotein samples. After washing, lipoproteins were eluted from the lipid removal agent with SDS loading buffer (Life Technologies, Grand Island, NY). For immunoblotting, equal volumes of sample were loaded onto a 4–12% Bis-Tris gel (Life Technologies) and electrophoresed at 200 V in MOPS buffer. Proteins were transferred to polyvinylidene difluoride membrane (Life Technologies), using a Pierce G2 Fast Blotter (Thermo Scientific, Rockford, IL) for 15 min at 25 V and 3.2 A. Following the protein transfer, membranes were blocked with 5% milk and 3% BSA. Membranes were stained sequentially with the following antibodies: mouse anti-mouse apoB-100/48 (5  $\mu$ g/ml, 1:500) (kindly provided by Dr. Steve Young), rabbit anti-mouse apoA-I serum (1:2,000), and apoE serum (1:1,000) (Meridian Life Science, Inc., Memphis, TN). Primary antibodies were detected with the appropriate secondary antibody conjugated to HRP (Abcam, Cambridge, MA). Staining was visualized on an Omega Lum C (Aplegen, San Francisco, CA) using the WesternBright Quantum detection kit (Advansta Inc., Menlo Park, CA). FPLC fractions were pooled into three peaks corresponding to VLDL, LDL, and HDL and labeled 1, 2, and 3, respectively (Fig. 2). Lipoproteins were concentrated using lipid removal agent (Sigma). Samples were digested with trypsin at 37°C overnight. The digest was separated with a nanoLC system and detected in data-dependent analysis mode on an LTQ Orbitrap Elite or Fusion (Thermo Fisher Scientific, San Jose, CA). Relative abundance of each protein of interest was estimated based on its total spectrum counts across the fractions/samples.

The VLDL triglyceride production study was carried out as previously described (34). Plasma from fasting mice was collected following injection with Triton WR-1339 at 0, 30, 60, 120, and 180 min postinjection.

### RNA isolation and gene expression analysis

All reagents used in real time PCR experiments were obtained from Life Technologies unless otherwise noted. RNA was isolated

from frozen liver tissue using RNeasy<sup>®</sup>-LysR. RNA was extracted from thawed tissue, using Trizol, and reverse transcription was carried out using Moloney murine leukemia virus reverse transcriptase oligo(dT) primers, and 1 µg of total RNA. Gene expression analysis was performed with TaqMan<sup>®</sup> Universal PCR Master Mix and commercially available primers for murine *ApoB*, *Hmgcr*, *Ldlr*, and *Pcsk9* on an ABI 7900. Values were normalized to murine *Actb* and then normalized to expression of each gene in the WT mice. Values are expressed as  $\log(2^{-\Delta\Delta CT})$ .

### Cholesterol efflux capacity and ex vivo LCAT activity

apoB-depleted serum was prepared by precipitation with polyethylene glycol (20%, v/v, in glycine buffer, pH 7.4). Global cholesterol efflux capacity of serum HDL samples was determined as described in detail elsewhere (35–37). In brief, global cholesterol efflux was measured using J774 mouse macrophage cells in the presence of cAMP. Cells were preincubated with [<sup>3</sup>H]cholesterol and ACAT inhibitor Sandoz 58-035 (but not preloaded with mass cholesterol) overnight. Cells were then incubated overnight in 0.2% BSA with cAMP. After washing, cells were incubated for 4 h with the serum HDL samples (apoB-depleted serum) added at 2.8% (v/v). [<sup>3</sup>H]cholesterol released to serum after 4 h was measured by liquid scintillation counting. Cholesterol efflux is expressed as the radiolabel released as a percentage of [<sup>3</sup>H]cholesterol within cells before addition of serum. All efflux values were corrected by subtracting the small amount of radioactive cholesterol released from cells incubated with serum-free medium. When indicated, J774 cells for some experiments were first loaded with Ac-LDL (180 µg/ml) for 72 h. Following cholesterol loading, these cells were incubated with 2.8% apoB-depleted serum overnight. TC was determined in cell layers and standardized to total protein as described below.

For determination of ex vivo LCAT activity, lipid was extracted from an aliquot of the efflux medium, and thin-layer chromatography was performed to quantitate the proportion of [<sup>3</sup>H]FC and [<sup>3</sup>H]cholesterol ester in the sample. Ex vivo LCAT activity is expressed as the proportion of [<sup>3</sup>H]cholesterol ester formed as a percentage of the total [<sup>3</sup>H]cholesterol released during the 4 h efflux period.

### Cellular cholesterol mass uptake

For mass cholesterol uptake assay,  $1.5 \times 10^6$  RAW cells (ATCC, Manassas, VA) were added to a 6-well tissue culture treated plate (Corning Inc., Corning, NY). Opti-MEM (Invitrogen) plus 3% mouse serum was added to the cells and incubated overnight. Cells were washed three times in PBS (Invitrogen), then lipids were extracted with 2:1 hexane:isopropanol solution. After removal of the organic solvent, protein from cells was extracted with 0.1 N NaOH/0.1% SDS. Protein concentration from each well was determined by BCA assay (Pierce, Rockford, IL). Lipids were resuspended in 100% ethanol, and levels of cholesterol were measured using the Amplex Red assay (Invitrogen).

Hepatic cell uptake was performed in Fu5AH rat hepatoma cells, as previously described (38), with the following modifications. Briefly, labeled media from the efflux assay were pooled and then applied to Fu5AH hepatoma cells. [<sup>3</sup>H]cholesterol uptake from serum, after incubation for 2 h, was measured by liquid scintillation counting. Cholesterol uptake is expressed as the radiolabel within cells as a percentage of [<sup>3</sup>H]cholesterol that was added to cells.

### Fluorescence-activated cell sorting analysis of platelets and erythrocytes

To detect the level of cholesterol in erythrocytes and platelets, 15 µl of whole blood was washed once with ice-cold PBS. Cells were resuspended in 80 µl of antibody solution and incubated at

room temperature for 20 min. After incubation, cells were fixed with 4% paraformaldehyde for 1 h at 4°C. Following fixation, cells were washed one time with PBS and resuspended in 500 µl of a 120 µg/ml filipin solution (Polysciences, Inc., Warrington, PA) supplemented with 2% dextran. Antibodies for erythrocytes and platelets, TER-119 and CD41 (BD Biosciences, San Jose, CA), respectively, were used at a 1/100 dilution. Cells were kept on ice until they could be analyzed by flow cytometry, using an LSRFortessa or FACsARIA (BD Biosciences).

To assess the level of reticulated platelets, cells were stained as previously described (39, 40). Briefly, 1 µl of whole blood was stained with antibodies against CD41, as described above. Following staining, the sample was diluted with 1 ml of PBS containing 100 ng/ml of thiazole orange (Sigma). Cells were kept on ice until they could be analyzed by flow cytometry, using an LSRFortessa (BD Biosciences).

### Analysis of atherosclerotic lesions

Following euthanasia, the vasculature was washed by perfusion through the heart with PBS. The aorta was then isolated from its origin in the heart to the ileal bifurcation. After removal of adventitial fat, the aorta was placed in 4% paraformaldehyde solution for 18 h. The fixed aorta was stained with a Sudan IV solution for 25 min, destained for 25 min in 80% ethanol, and washed in water. Then the aorta was cut longitudinally, embedded in glycerin, and sealed between a glass slides. Quantification of the area of the aortic plaques was performed with Image-Pro Plus version 4.1 software (Media Cybernetics, Inc., Bethesda, MD).

The evaluation of atherosclerosis in aortic valve leaflets was performed as previously described (41). Briefly, the heart and attached section of ascending aorta were dissected en bloc and embedded in OCT (Sakura Finetek, Torrance, CA). The aortic sinus was sectioned serially (10 µm intervals) using a cryostat (model CM3050 S; Leica Microsystems, GmbH, Wetzlar, Germany). Sections were fixed in a 4% paraformaldehyde solution for 15 min and stained for neutral lipids with Oil Red O (Poly Scientific R&D Corp., Bay Shore, NY). The images were acquired using a Leica DM 4000 B microscope and Leica DFC 500 camera (Leica Microsystems, GmbH). Five sections per animal were evaluated to calculate the area of lesions in the aortic sinus.

### Confocal and polarization microscopy

To visualize FC in tissues, fixed frozen tissue was stained with filipin (100 µg/ml) at room temperature. After staining, slides were mounted in a water-based mounting medium (Polysciences, Inc.). Tissue sections were examined using a HC-PL-IRAPO 40×/1.1 NA water immersion objective (WD = 0.6 mm) on a Leica TCS SP5-AOBS 5-channel confocal system (Leica Microsystems) equipped with multiline argon, diode 405 nm, 561 nm, HeNe 594 nm, and HeNe 633 nm visible lasers. Filipin fluorescence was detected using 405 nm excitation. Quantification of the intima area of the aorta that stained with filipin was performed in ImageJ (42). Cholesterol crystals were imaged using polarization microscopy (43) and appear white in photomicrographs.

### Statistical analysis

Results represent the mean ± SEM and all statistics were calculated using Prism 6 (GraphPad Software, Inc., La Jolla, CA). Groups were compared using a one- or two-way ANOVA as indicated. Post hoc analysis using Bonferroni's test was used to compare multiple groups. Statistics reported on each graph were calculated by comparing S<sup>-</sup>L<sup>+</sup> mice to each of the other strains or, when indicated, each strain was compared on a standard chow versus Western diet basis. All statistical comparisons are shown in supplementary Table 1.

## RESULTS

### LCAT alters plasma lipid and lipoprotein profiles in SR-BI-deficient mice

To test the hypothesis that increased expression of LCAT could overcome the cholesterol esterification defect in HDL and the FC enrichment in blood cells observed in *Scarab*( $-/-$ ) mice, the following lines of mice were purchased or created: 1) C57BL/6 (WT), 2)  $S^{-}L^{+}$ , 3)  $S^{-}L^{-}$ , and 4)  $S^{-}L^{++}$ . On a normal chow diet, all three strains of mice on the *Scarab*( $-/-$ ) background had higher TC than the WT mice, with the  $S^{-}L^{++}$  mice having the highest level of TC (Fig. 1A). Following 7 months on a high-fat diet, all mouse strains displayed an increase in plasma levels of TC, FC, cholesteryl esters, and phospholipids (Fig. 1A–D). Only  $S^{-}L^{+}$  and  $S^{-}L^{-}$  mice, however, showed increased levels of triglycerides after the Western diet (Fig. 1E). The majority of the increase in TC in the  $S^{-}L^{++}$  mice appears to be due to an increase in cholesteryl esters, presumably from increased esterification by LCAT. In contrast,  $S^{-}L^{+}$  and  $S^{-}L^{-}$  mice had higher levels of FC than cholesteryl esters on both the normal and the Western diet. The FC/TC ratio in plasma from WT mice was close to 0.25 on both the chow and the Western diet, whereas in  $S^{-}L^{+}$  mice, the ratio was between 0.5 and 0.6 (Fig. 1F), which is in agreement with previous reports (40). The  $S^{-}L^{-}$  mice had an even higher FC/TC ratio than the  $S^{-}L^{+}$  mice on both diets, between 0.88 and 0.62.

Interestingly, LCAT overexpression in the  $S^{-}L^{++}$  mice was able to restore the altered FC/TC ratio due to *Scarab*( $-/-$ ) deficiency when on a normal chow diet and to limit the increase in the FC/TC to 0.36 following a Western diet (Fig. 1F). As expected, the  $S^{-}L^{-}$  mice had very low levels of cholesteryl esters on the chow diet due to

the absence of LCAT, but there was a significant increase in plasma cholesteryl esters after the Western diet, most likely from intracellular esterification by ACAT (44–46). As expected, cholesterol in WT mice was found mainly on HDL, but following the Western diet, a peak of cholesterol corresponding to LDL was also observed (Fig. 2A). As previously described (47), the  $S^{-}L^{+}$  mice had a marked increase in cholesterol in larger sized HDL fractions, and increased levels of cholesterol in peaks corresponding to VLDL and LDL after a Western diet (Fig. 2B). As expected, loss of LCAT resulted in an almost total loss of HDL and an accumulation of VLDL- and LDL-sized particles in  $S^{-}L^{-}$  mice (Fig. 2C).  $S^{-}L^{++}$  mice showed a similar lipoprotein distribution as the  $S^{-}L^{+}$  mice on the normal chow diet, but appeared to have a slightly larger HDL peak. Compared with the  $S^{-}L^{+}$  mice (Fig. 2B), the increased LCAT activity in the  $S^{-}L^{++}$  mice (Fig. 2D) appeared to cause a marked decrease in VLDL and LDL, and to significantly raise HDL.

By Western blot analysis, the large HDL in  $S^{-}L^{+}$  mice on the Western diet was enriched in apoE (Fig. 2B), as has been previously described (47). In the case of the  $S^{-}L^{-}$  mice (Fig. 2C), most of the apoE was found in larger size fractions corresponding to LDL and VLDL. The apolipoprotein distribution for the  $S^{-}L^{++}$  mice (Fig. 2D) was similar to the  $S^{-}L^{+}$  mice (Fig. 2B). The main difference was that apoE was found in larger size fractions that also contained apoB, suggesting that the front shoulder of the large HDL peak observed in these mice may also contain some apoB-containing lipoproteins. This was confirmed by agarose gel electrophoresis, which showed a small amount of LDL in  $S^{-}L^{++}$  mice. The  $S^{-}L^{-}$  mice, which had no HDL, had even more LDL/VLDL than the  $S^{-}L^{++}$  mice (supplementary Fig. 2). The same FPLC lipoprotein

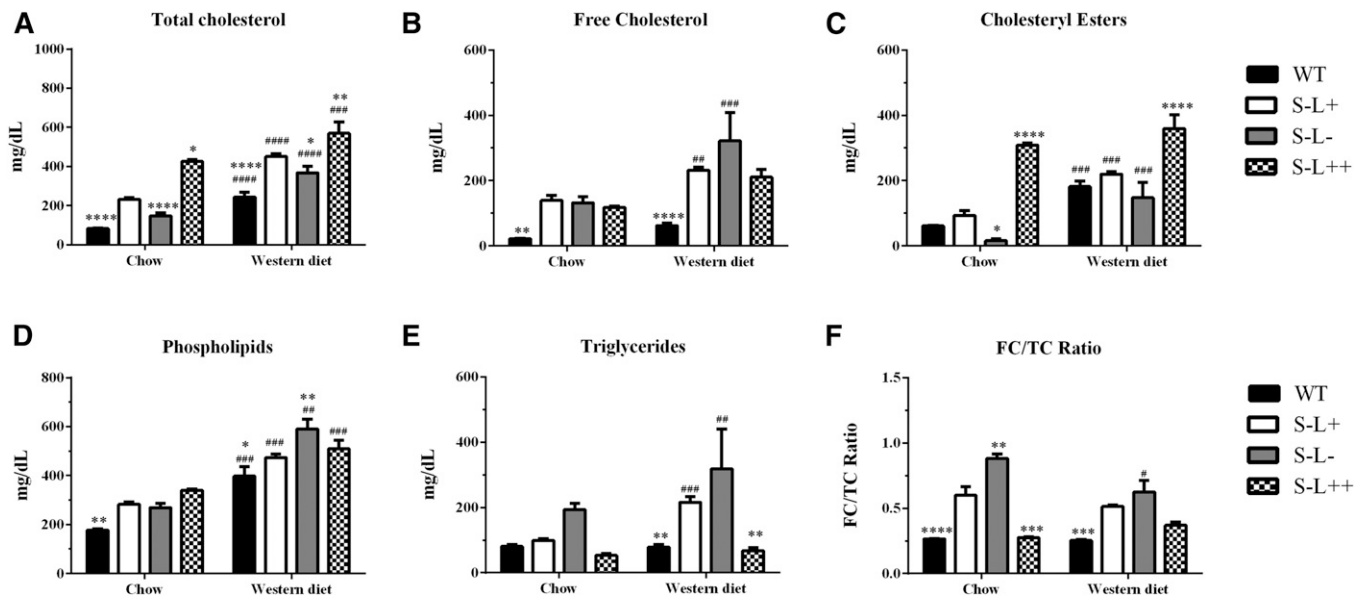


**Fig. 1.** Effect of LCAT on total plasma lipids and cholesterol esterification. A–F: Display levels of TC, FC, cholesterol ester, phospholipids, triglycerides, and FC/TC ratio, respectively, on normal chow or Western diet. *P* values were determined by a two-way ANOVA. The # denotes comparisons between normal and Western diet for each strain and \* denotes a comparison between  $S^{-}L^{+}$  mice and each strain on the same diet. \*,#*P* = 0.05; \*\*,##*P* = 0.01; \*\*\*,###*P* = 0.001; \*\*\*\*,####*P* = 0.0001; n = 6–8 mice per group.

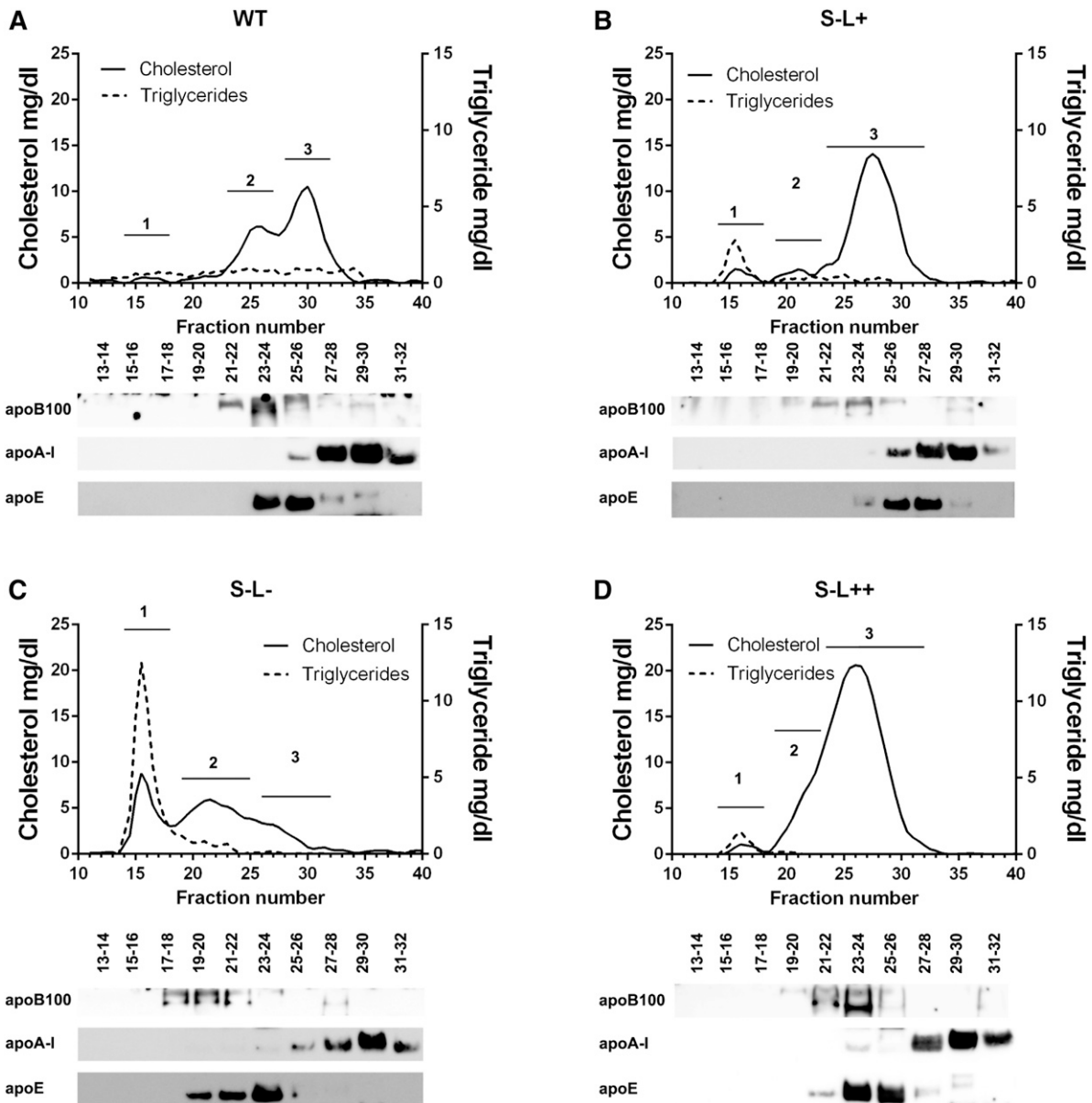


**Fig. 2.** FPLC profiles and characterization of peaks on a Western diet for 7 months. Graphs show FPLC profiles and corresponding Western blot analysis of WT (A),  $S^{-}L^{+}$  (B),  $S^{-}L^{-}$  (C), and  $S^{-}L^{++}$  (D) mice. The solid line denotes TC and the dashed line represents triglyceride values. Western blot analysis was performed on pooled fractions as indicated and probed with antibodies to apoB-100, apoA-I, and apoE. Plasma from four mice per group was pooled at each time point. Numbers 1, 2, 3 on FPLC graphs designate areas corresponding to VLDL, LDL, and HDL, respectively.

fractions were also analyzed for their protein content by LC-MS (supplementary Fig. 1, supplementary Table 2) and largely supported the findings from the Western blot analysis. In addition, it was found that LCAT was enriched in both HDL and LDL from  $S^{-}L^{++}$  mice and that HDL from these mice had either a restoration or an increase compared with WT mice in apoA-II, apoCs, and apoM, which were either decreased or not detected in HDL from  $S^{-}L^{-}$  mice.

#### Effect of LCAT on cholesterol efflux and uptake

As LCAT has been proposed to affect multiple steps in the RCT pathway, we investigated the ability of serum from the four lines of mice to promote cholesterol efflux from cells, to esterify cholesterol, and to donate cholesterol to liver cells

and macrophages (Fig. 3). Despite the relatively large differences in lipoprotein profiles of the four lines of mice, there were only minor differences in radiolabeled cholesterol efflux from J774 cells on the chow or Western diet, using apoB-depleted serum (Fig. 3A). Cholesterol efflux was also monitored from cholesterol-loaded J774 cells after treatment with apoB-depleted serum on a Western diet by monitoring FC and cholesteryl ester mass from cells (Fig. 3B). Compared with WT mice, cell lines treated with serum from all three lines of mice lacking *Scarab* ( $-/-$ ) had higher FC levels, but the levels were only statistically higher for the  $S^{-}L^{+}$  mice.

In addition to monitoring cholesterol efflux, we also measured the esterification of cholesterol in the conditioned media after cholesterol efflux (Fig. 3C). As

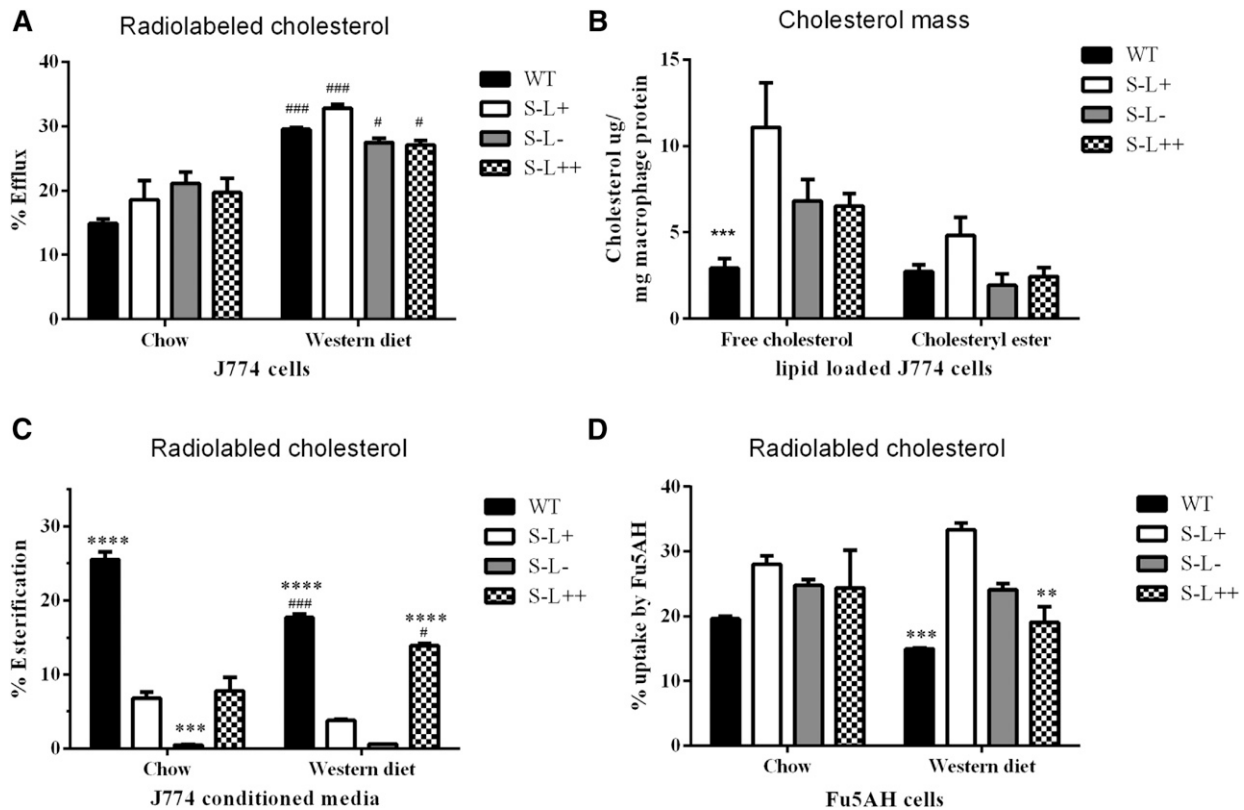


**Fig. 3.** Effect of LCAT on measures of cholesterol efflux. A: Efflux of radiolabeled cholesterol from J774 macrophages to apoB-depleted serum on normal chow or Western diet. B: Mass of cholesterol remaining in cholesterol-loaded J774 macrophages following incubation with apoB-depleted serum. C: Percent of radiolabeled cholesterol from conditioned media in (A) that was esterified during cholesterol efflux assay. D: Uptake of radiolabeled cholesterol from conditioned media in (A) by Fu5AH cells. *P* values were obtained by two-way ANOVA. The # denotes comparisons between normal and Western diet for each strain and \* denotes a comparison between S<sup>-</sup>L<sup>+</sup> mice and each strain. \*,#*P* = 0.05; \*\*,##*P* = 0.01; \*\*\*,###*P* = 0.001; \*\*\*\*,####*P* = 0.0001; *n* = 3 mice per group.

expected, there was no significant cholesterol esterification during the cholesterol efflux experiment in the S<sup>-</sup>L<sup>-</sup> mice that lack LCAT (Fig. 3C). The S<sup>-</sup>L<sup>+</sup> mice also had an approximate 75% reduction in esterification compared with WT mice (Fig. 3C), which is consistent with the observed decrease in their relative plasma cholesteryl ester content. This is most likely due to the fact that large HDL, which accumulates in these mice, is known to be a poor substrate for LCAT (48). Interestingly, apoB-depleted serum from WT and S<sup>-</sup>L<sup>+</sup> mice showed less esterification after being placed on the Western diet compared with chow. This is consistent with the observed increase in plasma FC in these mice on the Western diet (Fig. 1), indicating that the esterification of cholesterol by LCAT was less efficient on a high-fat diet. Similar results have been previously shown in *ApoE*(-/-) and *Ldlr*(-/-) mice (49). Increased expression of LCAT in S<sup>-</sup>L<sup>++</sup> mice resulted in a greater fraction of the effluxed cholesterol being esterified compared with the S<sup>-</sup>L<sup>+</sup> mice on the Western diet (Fig. 3C). Again, the decrease in esterification observed on the Western diet is likely due to the increased size of the HDL (48) (Fig. 2), but increased LCAT in the S<sup>-</sup>L<sup>++</sup> mice was able to largely overcome this defect. In fact, cholesterol esterification for the S<sup>-</sup>L<sup>++</sup> mice almost approached the level observed in WT mice when on a Western diet.

Conditioned medium containing radiolabeled cholesterol from the cell cholesterol efflux experiment in Fig. 3A was also used to assess cholesterol uptake into Fu5AH cells, a rat hepatoma cell line that abundantly expresses SR-BI (50). All three lines of mice lacking SR-BI showed an increase in cholesterol uptake compared with WT mice on a chow diet, but following a Western diet, serum from both WT and S<sup>-</sup>L<sup>++</sup> mice displayed a significant reduction in cholesterol uptake by cells compared with S<sup>-</sup>L<sup>+</sup> mice (Fig. 3D).

To explore the atherogenic potential of serum from these mice, we examined the ability of whole serum to donate cholesterol to macrophages, as previously described (51). Compared with WT mice, RAW macrophages incubated with serum from all three *Scarab*(-/-) mouse background strains showed an increase in cholesteryl ester mass accumulation, but no changes in FC (Fig. 4).

#### Effect of LCAT on hepatic gene expression and VLDL production

To better understand the mechanism behind the observed differences in the level of pro-atherogenic apoB-containing lipoproteins in the different mice (Fig. 2), we examined hepatic gene expression and VLDL production rate on the Western diet (Fig. 5). Interestingly, when compared with WT mice, liver cells from S<sup>-</sup>L<sup>-</sup> mice displayed a significant decrease in *Hmgcr*, *Ldlr*, and *Pcsk9*, and a

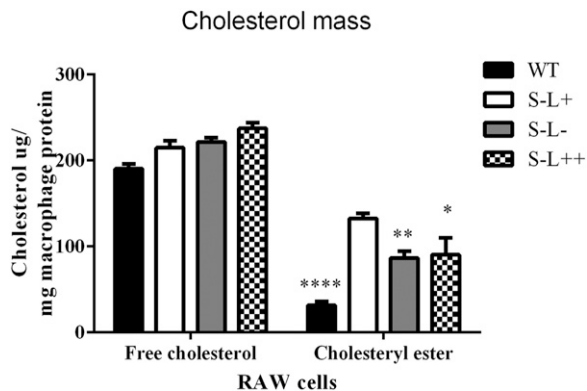


**Fig. 4.** Effect of LCAT on the atherogenic potential of serum. RAW cell uptake of cholesterol mass from whole serum. *P* values were obtained by two-way ANOVA. The # denotes comparisons between normal and Western diet for each strain and \* denotes a comparison between  $S^{-}L^{+}$  and each strain. \* $\#P = 0.05$ ; \*\* $\#\#P = 0.01$ ; \*\*\*\* $\#\#\#\#P = 0.0001$ ; *n* = 3 mice per group.

trend toward decreased *Apob* transcripts (Fig. 5A). Similar trends were observed in the other two *Scarab*( $-/-$ ) mouse strains, but did not reach statistical significance. The decrease in gene expression could possibly be compensatory due to the high level of VLDL observed in the plasma of  $S^{-}L^{-}$  mice. To determine whether there are differences in hepatic VLDL secretion, LPL activity was inhibited with Triton WR-1339 in fasting mice, and plasma levels of lipids

and lipoproteins were monitored over 3 h. All three of the *Scarab*( $-/-$ ) lines of mice displayed a similar lower rate of hepatic triglyceride-rich lipoprotein secretion compared with the WT mice (Fig. 5B). This suggests that the accumulation of VLDL and LDL observed in the  $S^{-}L^{-}$  mice (Fig. 2) is most likely due to decreased plasma clearance. Lastly, when the levels of FC were examined by FLPC in VLDL-sized fractions, we observed that  $S^{-}L^{-}$  mice had a greater than 8-fold increase in FC compared with  $S^{-}L^{+}$  mice (Fig. 5C). In contrast, almost all of the cholesterol on VLDL was esterified in WT and  $S^{-}L^{++}$  mice (Fig. 5C).

#### LCAT increases cell counts and alters the FC content of RBCs and platelets

Because it has previously been reported that *Scarab*( $-/-$ ) mice have abnormalities in their cholesterol content and number of RBCs and platelets (19, 32, 40), we examined the ability of LCAT to modulate these parameters. There were no significant differences observed in RBC counts in the four strains of mice on the chow diet. On the Western diet, however, both  $S^{-}L^{+}$  and  $S^{-}L^{-}$  mice showed a trend toward lower RBC counts compared with WT and  $S^{-}L^{++}$  mice, although the difference was not significant (Fig. 6A). When the FC content of RBCs was examined, these same mice showed a dramatic increase in FC on the Western diet (Fig. 6B). The increased expression of LCAT in the  $S^{-}L^{++}$  mice appeared to significantly blunt the increase in FC on RBCs (Fig. 6B).

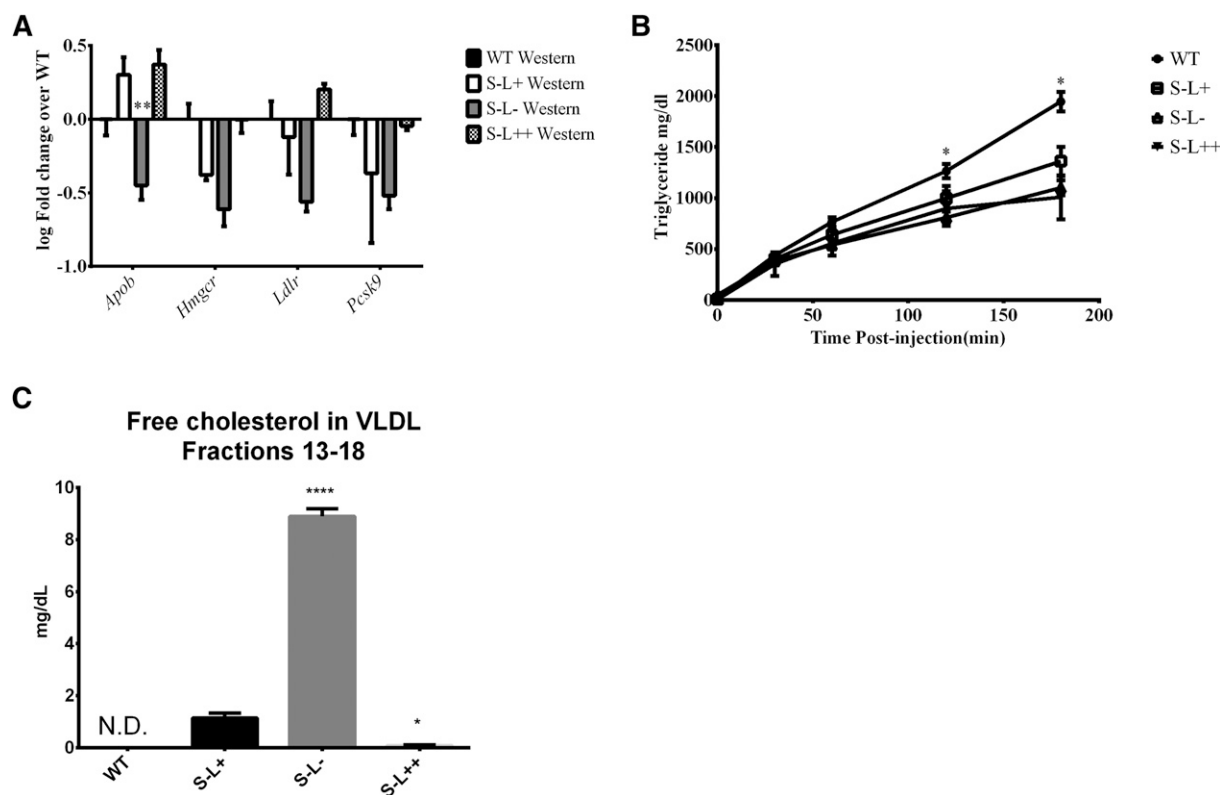


**Fig. 5.** Effect of LCAT on hepatic gene expression and VLDL secretion. A: Expression of key hepatic genes from livers of the indicated mice. All values normalized to WT animals (*n* = 4). B: Plasma triglyceride levels of mice after inhibition of LPL with Triton (*n* = 4). C: Concentration of FC on VLDL. *P* values were obtained by two-way ANOVA. The # denotes comparisons between normal and Western diet for each strain and \* denotes a comparison between  $S^{-}L^{+}$  and each strain. \* $\#P = 0.05$ ; \*\* $\#\#P = 0.01$ ; \*\*\*\* $\#\#\#\#P = 0.0001$ .

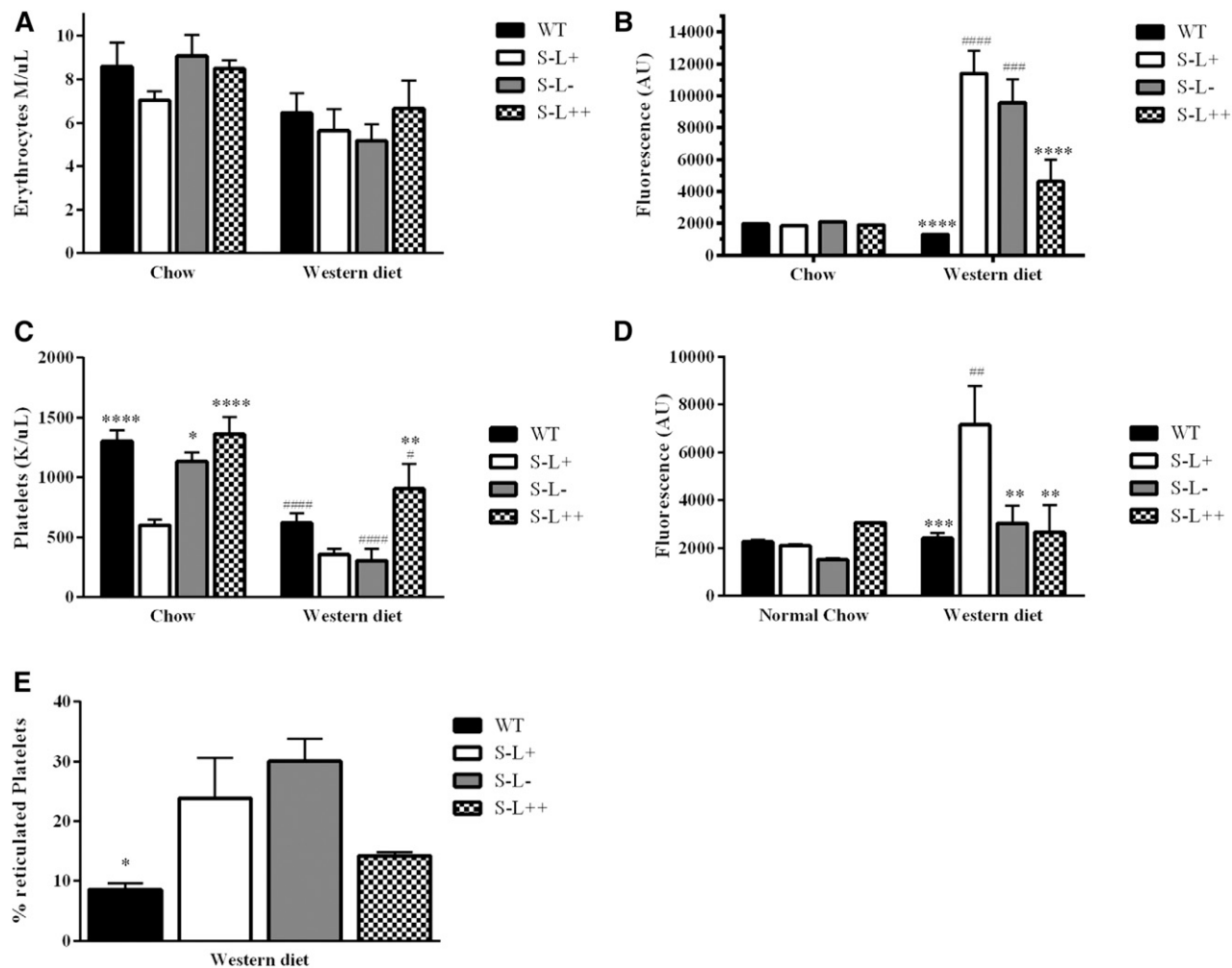


**Fig. 6.** Effect of LCAT on RBC and platelet counts and FC content. A: RBC counts of mice on chow or Western diet (7 months). B: RBC FC content, as determined by filipin staining of mice on chow or Western diet (7 months). C: Platelet counts of mice on chow or Western diet (7 months). D: Platelet FC content, as determined by filipin staining of mice on chow or Western diet (7 months). E: Percentage of reticulated platelets as determined by thiazole orange staining on the Western diet ( $n = 6$  or  $n = 10-12$  on chow or Western diet, respectively).  $P$  values were obtained by two-way ANOVA. The # denotes comparisons between normal and Western diet for each strain and \* denotes a comparison between  $S^{-}L^{+}$  and each strain. \*,# $P = 0.05$ ; \*\*,## $P = 0.01$ ; \*\*\*,### $P = 0.001$ ; \*\*\*\*,#### $P = 0.0001$ .

On the chow diet,  $S^{-}L^{+}$  mice had an approximate 50% decrease in platelet counts (Fig. 6C), as previously described (40), and either increasing or decreasing LCAT levels normalized platelet counts for the  $S^{-}L^{++}$  and  $S^{-}L^{-}$  mice, respectively. On the Western diet, all strains of mice displayed a significant decrease in platelet counts, but increased expression of LCAT in the  $S^{-}L^{++}$  mice was able to blunt the decrease in platelets. FC levels in platelets, as assessed by filipin staining, showed minimal differences between strains on the chow diet (Fig. 6D), but on the Western diet,  $S^{-}L^{+}$  mice displayed an enrichment of FC in platelets, as has been previously described (40). The  $S^{-}L^{-}$  mice did not show any enrichment of cholesterol, but these mice and the  $S^{-}L^{+}$  mice showed a 3.4- and 2.7-fold increased rate of platelet production, respectively, over WT mice, as assessed by staining for nucleic acids with thiazole orange (Fig. 6E), suggesting that differences in the rate of platelet clearance may alter the accumulation of cholesterol-rich platelets in the blood compartment.

### LCAT protects *Scarab(-/-)* mice from developing atherosclerosis

As mice lacking SR-BI have been reported to have increased atherosclerosis in their aortic root (27) and also in their aorta by en face analysis when crossed with *ApoE(-/-)* or *Ldlr(-/-)* mice (23, 27, 52), we determined whether LCAT could modulate diet-induced atherosclerosis. After seven months on a Western diet, only a limited degree of atherosclerosis, as measured by en face analysis, was observed in any of the mouse strains except for the  $S^{-}L^{-}$  mice, which had more than a 20-fold increase in atherosclerosis compared with  $S^{-}L^{+}$  mice (Fig. 7A, D). Examination of the aortic root revealed that  $S^{-}L^{+}$  mice had a trend toward increased atherosclerosis compared with WT mice, similar to what was previously reported (27), but in our study this did not reach statistical significance (Fig. 8A, C). The absence of LCAT in the  $S^{-}L^{-}$  mice resulted in a further increase in atherosclerosis above  $S^{-}L^{+}$  mice; however, this was also not statistically significant above the levels seen in  $S^{-}L^{+}$  mice, but was significantly increased ( $P < 0.05$ ) when compared with WT mice



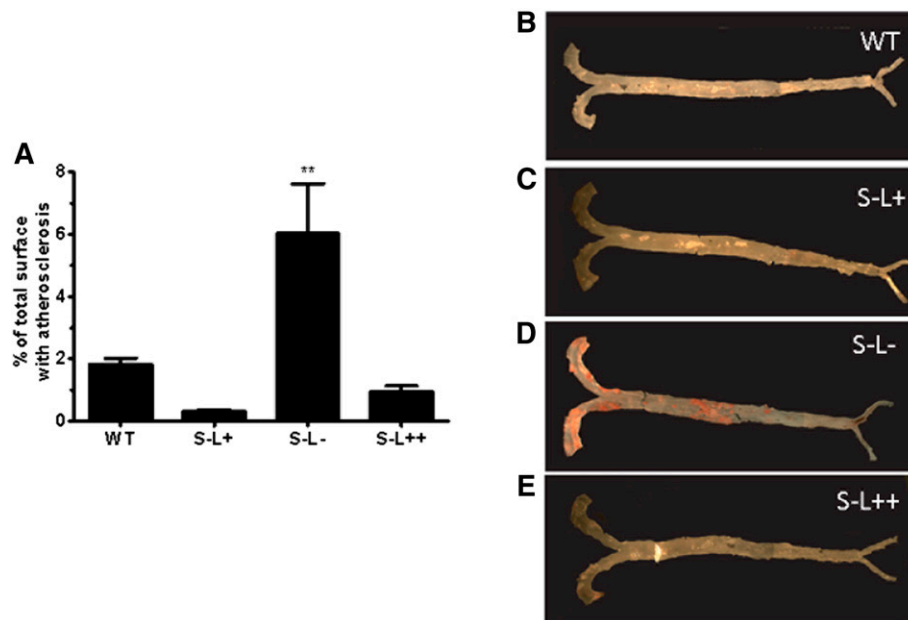


**Fig. 7.** Effect of SR-BI and LCAT expression on diet-induced atherosclerosis. Whole aortas from mice following 7 months on a Western diet were stained with Sudan IV to visualize lipid deposits. A:  $S^{-}L^{-}$  mice displayed increased atherosclerosis following 7 months on a Western diet, while  $S^{-}L^{+}$  and  $S^{-}L^{++}$  mice did not display any increase in atherosclerosis. B–E: Representative images of whole aorta from WT,  $S^{-}L^{+}$ ,  $S^{-}L^{-}$ ,  $S^{-}L^{++}$ , respectively.  $P$  values were determined by one-way ANOVA.  $**P \leq 0.01$ ;  $n = 9$ – $12$  mice per group.

(Fig. 8A, D). In contrast, relatively small amounts of atherosclerosis were detected in the aortic root of  $S^{-}L^{++}$  mice and were similar to those observed in WT mice.

Because recent reports have postulated that cholesterol crystals derived from FC may contribute to the initiation of

atherosclerosis (27, 53, 54), we examined the aortic sinus of these mice for the presence of cholesterol crystals by polarized light (Fig. 9B–E). We found abundant FC crystals in the lesions of both  $S^{-}L^{-}$  and  $S^{-}L^{+}$  mice, whereas cholesterol crystals were undetectable in WT and  $S^{-}L^{++}$

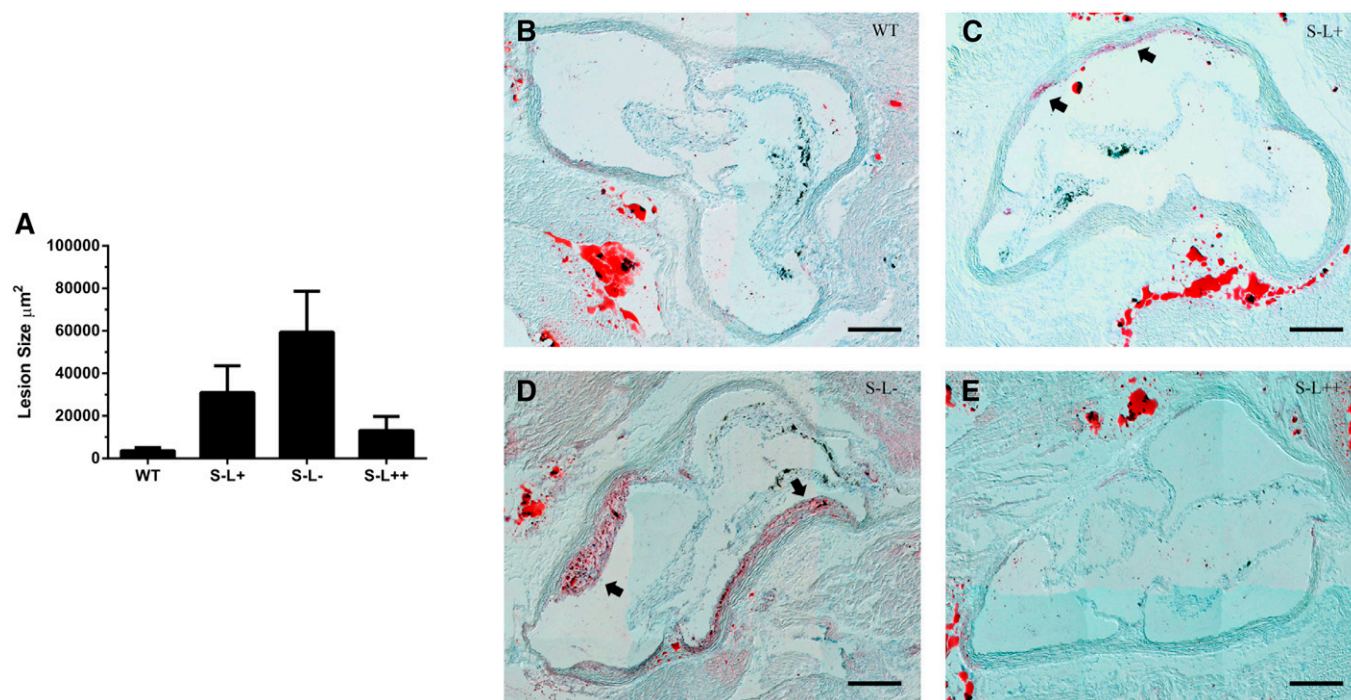


**Fig. 8.** Effect of LCAT expression on diet-induced atherosclerosis. Atherosclerosis was assessed in the aortic root by Oil Red O staining. A: Loss LCAT exacerbates atherosclerosis while overexpression of LCAT prevents atherosclerosis in *Scarab* ( $-/-$ ) mice. B–E: Representative images of aortic sinus from WT,  $S^{-}L^{+}$ ,  $S^{-}L^{-}$ , and  $S^{-}L^{++}$  mice, respectively. Arrows indicate atherosclerotic plaque. Scale bar indicates 200  $\mu\text{m}$ .  $*P < 0.05$  ( $n = 8$  per group).

mice (Fig. 9B–E). Interestingly, in the intimal regions of  $S^{-}L^{-}$  mice, where cholesterol crystals were observed, abundant staining was also observed for FC, as determined by filipin staining (Fig. 9A).

## DISCUSSION

Results from this study reveal that modulating the expression of LCAT in mice lacking the SR-BI receptor can

have a profound effect on numerous parameters and pathways related to lipoprotein metabolism and atherosclerosis. SR-BI deficiency is known to result in an increase of large HDL particles enriched in FC (23, 55, 56), but we found that increased LCAT was largely able to correct this phenotype (Fig. 1). Overexpression of LCAT in *Scarb*( $-/-$ ) mice resulted in a significant decrease in the fraction of unesterified cholesterol, whereas the loss of LCAT in the  $S^{-}L^{-}$  mice resulted in an almost total loss of HDL and a marked increase in unesterified cholesterol in plasma.

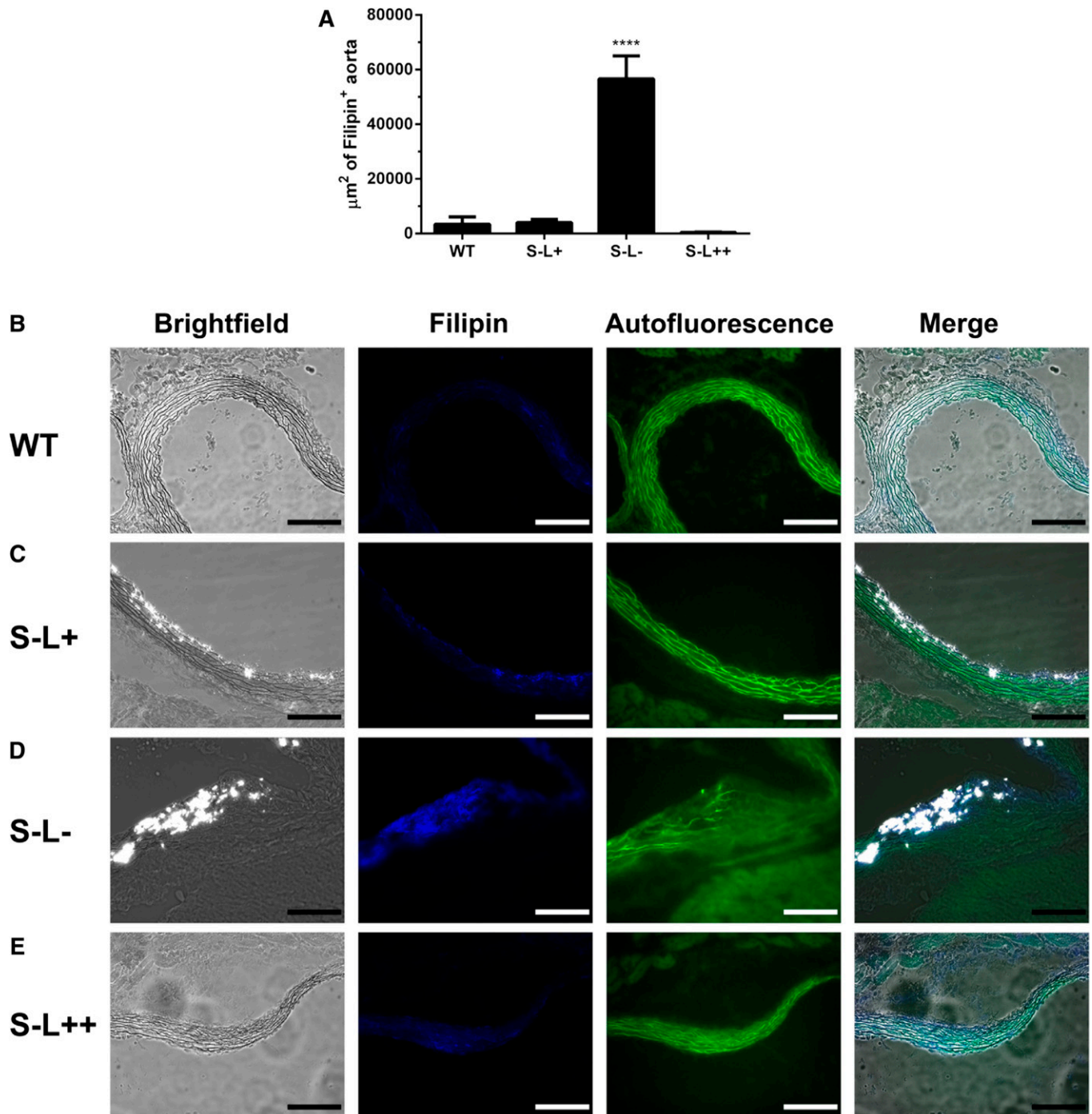


**Fig. 9.** Effect of LCAT on FC in the aortic sinus. A: Amount of FC in the intima of the aortic sinus was assessed by filipin staining. B–E: Representative images of cholesterol crystals detected by polarized light and the amount of FC detected by filipin stain in the aortic sinus. Scale bar indicates 100  $\mu\text{m}$ . \*\*\*\* $P < 0.0001$  ( $n = 4$  per group).

The loss of HDL in  $S^{-}L^{-}$  mice was also associated with a corresponding marked increase in pro-atherogenic LDL- and VLDL-sized particles. Interestingly, although the  $S^{-}L^{-}$  mice did not show an increase in TC compared with the other two strains of mice lacking the SR-BI receptor, they exhibited the most atherosclerosis. In contrast, the  $S^{-}L^{+}$  mice, which had the highest level of TC, were protected from diet-induced atherosclerosis, most likely because, unlike the  $S^{-}L^{-}$  mice, they had a decrease in cholesterol-containing pro-atherogenic lipoproteins, such as VLDL- and LDL-sized particles, and the majority of their cholesterol was on HDL (Fig. 2). Consistent with our data, it has been shown in *Ldlr*( $-/-$ ) mice that the level of VLDL-cholesterol (VLDL-C) is the best predictor of atherosclerosis (57, 58).

Although many epidemiologic studies have linked elevated levels of HDL-C to a decreased atherosclerotic risk (59, 60), there is evidence in some settings that elevated levels of HDL can in fact be detrimental (61–64). To date, the mixed results seen in the trials using CETP inhibitors (65) and niacin (66, 67) also suggest that simply elevating the cholesterol content of HDL does not necessarily improve cardiovascular outcomes (65). It was previously demonstrated that *Scarab*( $-/-$ ) mice, which have very high levels of HDL-C, in fact, develop more atherosclerosis (27, 28, 47, 52). Consistent with these observations, assays of HDL function, such as cholesterol efflux, may, in fact, be more predictive than HDL-C levels for cardiovascular risk (68). In this study, LCAT may perhaps be exerting its positive anti-atherogenic effect, at least in part, through modulation of HDL function. In support of this hypothesis, we found that LCAT overexpression normalized the FC/TC ratio (Fig. 1). This is in contrast to work previously published by Yesilaltay et al. (69), which found overexpression of LCAT in mice on a *Scarab*( $-/-$ ) background was not able to normalize the FC/TC ratio. The differences between our results and theirs are likely due to the much greater increase in LCAT expression in our mice compared with the previous study (31, 70).

Besides its effect on the FC/TC ratio, LCAT's effect on the lipoprotein distribution likely plays a role in its ability to modulate atherosclerosis development. Our observation of increased pro-atherogenic lipoproteins on a Western diet in mice lacking the SR-BI receptor (Fig. 2) is consistent with previously reported values (23, 27, 71), and loss of LCAT expression greatly exacerbated the increase in pro-atherogenic particles, particularly VLDL. This was observed by FPLC as an increase in the cholesterol peak corresponding to VLDL (Fig. 2), but could also be observed in  $S^{-}L^{+}$  and  $S^{-}L^{-}$  mice as an increase in the level of triglycerides in plasma (Fig. 1), which are largely transported by pro-atherogenic lipoproteins. It is quite striking that overexpression of LCAT was able to block this increase in both triglycerides and atherogenic particles. As shown in the experiment in which LPL was inhibited with Triton (Fig. 5), the increase in plasma levels of VLDL and LDL in the  $S^{-}L^{+}$  and  $S^{-}L^{-}$  mice were most likely due to decreased clearance. Decreased hepatic expression of the LDL receptor gene, particularly in the  $S^{-}L^{-}$  mice, could also have

contributed to these findings. Alternatively, the increased FC content of lipoproteins and the redistribution of LPL-modulating proteins such as apoC-II and apoC-III, which have been described to occur in familial LCAT deficiency (7, 8), could also account for the decreased lipolysis and clearance of apoB-containing lipoproteins. The results from this study are also consistent with previous animal models of either increased or decreased LCAT expression, which have shown that the effect of LCAT on the level of pro-atherogenic apoB-containing particles is the best predictor of whether LCAT promotes or decreases atherosclerosis in a given animal model (7, 8).

Surprisingly, modulation of LCAT expression did not seem to have a major impact on HDL function, as measured by an in vitro radiolabeled cholesterol efflux assay from macrophages, using apoB-depleted serum as the acceptor. It has been previously shown, however, that in vitro cholesterol efflux assays are relatively unaffected by the presence or absence of LCAT, because of the relatively low unphysiologic ratio of donor membranes to acceptor particles used in these studies (3). Using RBCs as a cholesterol donor, only at relatively high concentrations (hematocrit >15%), much higher than the ratio of donor membranes to acceptor particles typically used in in vitro cholesterol efflux assays, was LCAT shown to promote cholesterol efflux (3). We did observe, however, that a much greater fraction of the radiolabeled cholesterol effluxed from the macrophage cell line during the in vitro efflux study was esterified in the conditioned media containing serum from  $S^{-}L^{+}$  mice (Fig. 3B). Based on human tracer studies (4), approximately 80% of esterified cholesterol is returned to the liver as compared with only 4% of FC (2), which suggests that the esterification of cholesterol by LCAT should ultimately lead to increased hepatic excretion of cholesterol.

When we monitored bidirectional flux of cholesterol by measuring cholesterol mass in J744 macrophage cells (Fig. 3B), we found that incubation of apoB-depleted serum from all three strains of mice lacking SR-BI resulted in higher levels of FC than what we found with WT mice. This suggests that the large HDL that accumulates in the absence of SR-BI may, in fact, promote the net delivery of cholesterol to cells, possibly by the SR-BI receptor present on the J744 cells (72). Similarly, we observed (Fig. 3D) an increase in cholesterol uptake by Fu5AH cells, which also abundantly express SR-BI (50), when incubated with apoB-depleted serum from the three lines of mice lacking SR-BI. This again could be due to cellular uptake of cholesterol from HDL.


RBCs from LCAT-overexpressing mice on a Western diet had decreased levels of FC (Fig. 6). By lowering the amount of FC on lipoproteins, LCAT could be reducing the amount of FC that can passively exchange with RBCs (2). In general, increased levels of FC in cells have been shown to be pro-inflammatory and cytotoxic (11, 73), and result in increased atherosclerosis (74). RBCs themselves have also been shown to remove excess cholesterol from peripheral cells by a countercurrent-like exchange mechanism

and deliver it to the liver for excretion (13). The enrichment of FC on RBCs in the  $S^{-}L^{-}$  mice could thus potentially interfere with this process and could also lead to increased atherosclerosis. RBCs themselves have also been proposed as a possible source of cholesterol in plaque (15, 16).

Decreased LCAT activity in the  $S^{-}L^{+}$  and  $S^{-}L^{-}$  mice also appeared to be correlated with decreased platelet counts, and in the case of the  $S^{-}L^{+}$  mice, cholesterol enrichment of platelets (Fig. 6). A higher rate of platelet production was also observed for both the  $S^{-}L^{+}$  and  $S^{-}L^{-}$  mice despite their lower platelet counts, suggesting that these mice must have a higher rate of platelet turnover. Cholesterol enrichment of platelets is known to lead to increased platelet aggregation (20, 22, 75, 76), which could account for the lower platelet counts in the  $S^{-}L^{+}$  and  $S^{-}L^{-}$  mice. This process may also limit the accumulation of cholesterol-enriched platelets in blood due to their selective removal. We observed that the  $S^{-}L^{-}$  mice had much larger spleens than the  $S^{-}L^{+}$  mice (data not shown), which could account for the greater removal of cholesterol-rich platelets in these mice (Fig. 5D, E). Thrombosis from platelet aggregation also contributes to the development of atherosclerotic plaque (77).

A significant amount of atherosclerosis was only detected in the mice with decreased LCAT activity and an increase in the FC/TC ratio, namely the  $S^{-}L^{+}$  and  $S^{-}L^{-}$  mice (Figs. 7, 8). The difference we observed in the degree of atherosclerosis in the en face compared with the aortic root in the  $S^{-}L^{+}$  mice (Figs. 7, 8) is most likely due to differences in disease propensity in different anatomic locations, with plaque usually first developing in the aortic root before other locations. Cholesterol crystals, which are now thought to play a role in the early initiation of the atherosclerosis process (53), were also detected in the plaques of both  $S^{-}L^{+}$  and  $S^{-}L^{-}$  mice (Fig. 9). The increase in the FC/TC ratio on lipoproteins could promote cholesterol crystal formation when they enter the plaque, and could also account for the increase in FC staining by filipin in the  $S^{-}L^{-}$  mice (Fig. 9).

A limitation of our study is that the mice used in this study, unlike humans, did not contain CETP. Previous studies, however, have shown that CETP expression in mice can lower serum cholesterol in LCAT-Tg mice (78), and that CETP expression can protect *Scarab*( $-/-$ ) mice from the development of atherosclerosis (79). Interestingly, mice that overexpress LCAT are at increased risk of developing atherosclerosis on both the *Ldlr*( $-/-$ ) and *Apoe*( $-/-$ ) background (80, 81), but expression of CETP in these models has been shown to ameliorate the development of atherosclerosis (78). In contrast, LCAT overexpression in rabbits, which express CETP, protected against diet-induced atherosclerosis (82). Based on these results, it is possible that a greater atheroprotective effect from LCAT could be observed in *Scarab*( $-/-$ ) mice that express CETP, but this will have to be tested in future studies. Another potential limitation in our study is the mixed genetic background of the  $S^{-}L^{+}$  mice, which could be another source of variation in our study.

In summary, increased LCAT expression in *Scarab*( $-/-$ ) mice was found to lead to an anti-atherogenic lipoprotein phenotype and reduced diet-induced atherosclerosis. Further work is needed, however, to fully understand how LCAT affects the overall functionality of HDL in *Scarab*( $-/-$ ) mice and its role in RCT, as well as in other potential anti-atherogenic pathways. 

The authors thank Ann Williams and Heidi Mariani from the Flow Cytometry Core of the National Heart, Lung, and Blood Institute.

## REFERENCES

1. Kunnen, S., and M. Van Eck. 2012. Lecithin:cholesterol acyltransferase: old friend or foe in atherosclerosis? *J. Lipid Res.* **53**: 1783–1799.
2. Schwartz, C. C., J. M. VandenBroek, and P. S. Cooper. 2004. Lipoprotein cholesteryl ester production, transfer, and output in vivo in humans. *J. Lipid Res.* **45**: 1594–1607.
3. Czarnecka, H., and S. Yokoyama. 1996. Regulation of cellular cholesterol efflux by lecithin:cholesterol acyltransferase reaction through nonspecific lipid exchange. *J. Biol. Chem.* **271**: 2023–2028.
4. Schwartz, C. C., L. A. Zech, J. M. VandenBroek, and P. S. Cooper. 1993. Cholesterol kinetics in subjects with bile fistula. Positive relationship between size of the bile acid precursor pool and bile acid synthetic rate. *J. Clin. Invest.* **91**: 923–938.
5. Shamburek, R. D., L. A. Zech, P. S. Cooper, J. M. Vandenbroek, and C. C. Schwartz. 1996. Disappearance of two major phosphatidylcholines from plasma is predominantly via LCAT and hepatic lipase. *Am. J. Physiol.* **271**: E1073–E1082.
6. Chen, Z., S. P. Wang, M. L. Krsmanovic, J. Castro-Perez, K. Gagen, V. Mendoza, R. Rosa, V. Shah, T. He, S. J. Stout, et al. 2012. Small molecule activation of lecithin cholesterol acyltransferase modulates lipoprotein metabolism in mice and hamsters. *Metabolism.* **61**: 470–481.
7. Rousset, X., R. Shamburek, B. Vaisman, M. Amar, and A. T. Remaley. 2011. Lecithin cholesterol acyltransferase: an anti- or pro-atherogenic factor? *Curr. Atheroscler. Rep.* **13**: 249–256.
8. Rousset, X., B. Vaisman, M. Amar, A. A. Sethi, and A. T. Remaley. 2009. Lecithin: cholesterol acyltransferase—from biochemistry to role in cardiovascular disease. *Curr. Opin. Endocrinol. Diabetes Obes.* **16**: 163–171.
9. Shamburek, R. D., L. Freeman, M. Sampson, R. Bakker-Arkema, B. Krause, B. Auerbach, R. Homan, A. Shamburek, C. Schwartz, M. Amar, et al. 2013. Human enzyme replacement therapy in a patient with familial lecithin cholesterol acyltransferase deficiency: rapid appearance of normal appearing HDL. *Circulation.* **128**: A18673.
10. Kellner-Weibel, G., W. G. Jerome, D. M. Small, G. J. Warner, J. K. Stoltenborg, M. A. Kearney, M. H. Corjay, M. C. Phillips, and G. H. Rothblat. 1998. Effects of intracellular free cholesterol accumulation on macrophage viability: a model for foam cell death. *Arterioscler. Thromb. Vasc. Biol.* **18**: 423–431.
11. Warner, G. J., G. Stoudt, M. Bamberger, W. J. Johnson, and G. H. Rothblat. 1995. Cell toxicity induced by inhibition of acyl coenzyme A:cholesterol acyltransferase and accumulation of unesterified cholesterol. *J. Biol. Chem.* **270**: 5772–5778.
12. Nicholls, S. J., I. Sipahi, J. Andrews, K. Wolski, P. Schoenhagen, T. Crowe, M. Y. Desai, E. M. Tuzcu, and S. E. Nissen. 2006. Proatherogenic impact of the ACAT inhibitor pactimibe in patients with coronary artery disease and multiple risk factors: insights from the ACTIVATE study. *Circulation.* **114**: II-224.
13. Hung, K. T., S. Z. Berisha, B. M. Ritchey, J. Santore, and J. D. Smith. 2012. Red blood cells play a role in reverse cholesterol transport. *Arterioscler. Thromb. Vasc. Biol.* **32**: 1460–1465.
14. Lin, H. L., X. S. Xu, H. X. Lu, L. Zhang, C. J. Li, M. X. Tang, H. W. Sun, Y. Liu, and Y. Zhang. 2007. Pathological mechanisms and dose dependency of erythrocyte-induced vulnerability of atherosclerotic plaques. *J. Mol. Cell. Cardiol.* **43**: 272–280.
15. Tziakas, D., G. Chalikias, A. Grapsa, T. Gioka, I. Tentas, and S. Konstantinides. 2012. Red blood cell distribution width: a strong

- prognostic marker in cardiovascular disease: is associated with cholesterol content of erythrocyte membrane. *Clin. Hemorheol. Microcirc.* **51**: 243–254.
16. Tziakas, D. N., J. C. Kaski, G. K. Chalikias, C. Romero, S. Fredericks, I. K. Tentas, A. X. Kortsaris, D. I. Hatseras, and D. W. Holt. 2007. Total cholesterol content of erythrocyte membranes is increased in patients with acute coronary syndrome: a new marker of clinical instability? *J. Am. Coll. Cardiol.* **49**: 2081–2089.
  17. Vayá, A., M. Martínez Triguero, E. Réganon, V. Vila, V. Martínez Sales, E. Solá, A. Hernández Mijares, and A. Ricart. 2008. Erythrocyte membrane composition in patients with primary hypercholesterolemia. *Clin. Hemorheol. Microcirc.* **40**: 289–294. [Erratum. 2009. *Clin. Hemorheol. Microcirc.* **41**: 149.]
  18. Cooper, R. A., J. R. Durocher, and M. H. Leslie. 1977. Decreased fluidity of red cell membrane lipids in abetalipoproteinemia. *J. Clin. Invest.* **60**: 115–121.
  19. Holm, T. M., A. Braun, B. L. Trigatti, C. Brugnara, M. Sakamoto, M. Krieger, and N. C. Andrews. 2002. Failure of red blood cell maturation in mice with defects in the high-density lipoprotein receptor SR-BI. *Blood*. **99**: 1817–1824.
  20. Shattil, S. J., J. S. Bennett, R. W. Colman, and R. A. Cooper. 1977. Abnormalities of cholesterol-phospholipid composition in platelets and low-density lipoproteins of human hyperbetalipoproteinemia. *J. Lab. Clin. Med.* **89**: 341–353.
  21. Knöfler, R., T. Urano, T. Taminato, T. Yoshimi, T. Nakano, K. Nakajima, Y. Takada, and A. Takada. 1995. Daily variation of serum lipids in relation to the circadian rhythm of platelet aggregation in healthy male persons. *Clin. Chim. Acta.* **239**: 109–119.
  22. Shattil, S. J., R. Anaya-Galindo, J. Bennett, R. W. Colman, and R. Cooper. 1975. Platelet hypersensitivity induced by cholesterol incorporation. *J. Clin. Invest.* **55**: 636–643.
  23. Trigatti, B., H. Rayburn, M. Viñals, A. Braun, H. Miettinen, M. Penman, M. Hertz, M. Schrenzel, L. Amigo, A. Rigotti, et al. 1999. Influence of the high density lipoprotein receptor SR-BI on reproductive and cardiovascular pathophysiology. *Proc. Natl. Acad. Sci. USA.* **96**: 9322–9327.
  24. Arai, T., F. Rinninger, L. Varban, V. Fairchild-Huntress, C. P. Liang, W. Chen, T. Seo, R. Deckelbaum, D. Huszar, and A. R. Tall. 1999. Decreased selective uptake of high density lipoprotein cholesteryl esters in apolipoprotein E knock-out mice. *Proc. Natl. Acad. Sci. USA.* **96**: 12050–12055.
  25. Braun, A., B. L. Trigatti, M. J. Post, K. Sato, M. Simons, J. M. Edelberg, R. D. Rosenberg, M. Schrenzel, and M. Krieger. 2002. Loss of SR-BI expression leads to the early onset of occlusive atherosclerotic coronary artery disease, spontaneous myocardial infarctions, severe cardiac dysfunction, and premature death in apolipoprotein E-deficient mice. *Circ. Res.* **90**: 270–276.
  26. Kozarsky, K. F., M. H. Donahue, J. M. Glick, M. Krieger, and D. J. Rader. 2000. Gene transfer and hepatic overexpression of the HDL receptor SR-BI reduces atherosclerosis in the cholesterol-fed LDL receptor-deficient mouse. *Arterioscler. Thromb. Vasc. Biol.* **20**: 721–727.
  27. Van Eck, M., J. Twisk, M. Hoekstra, B. T. Van Rij, C. A. C. Van der Lans, I. S. T. Bos, J. K. Kruijt, F. Kuipers, and T. J. C. Van Berkel. 2003. Differential effects of scavenger receptor BI deficiency on lipid metabolism in cells of the arterial wall and in the liver. *J. Biol. Chem.* **278**: 23699–23705.
  28. Yu, H., W. Zhang, P. G. Yancey, M. J. Koury, Y. Zhang, S. Fazio, and M. F. Linton. 2006. Macrophage apolipoprotein E reduces atherosclerosis and prevents premature death in apolipoprotein E and scavenger receptor-class BI double-knockout mice. *Arterioscler. Thromb. Vasc. Biol.* **26**: 150–156.
  29. Ma, K., T. Forte, J. D. Otvos, and L. Chan. 2005. Differential additive effects of endothelial lipase and scavenger receptor-class B type I on high-density lipoprotein metabolism in knockout mouse models. *Arterioscler. Thromb. Vasc. Biol.* **25**: 149–154.
  30. Barter, P. J., G. J. Hopkins, and L. Gorjatschko. 1985. Lipoprotein substrates for plasma cholesterol esterification: influence of particle size and composition of the high density lipoprotein subfraction 3. *Atherosclerosis.* **58**: 97–107.
  31. Vaisman, B. L., H. G. Klein, M. Rouis, A. M. Berard, M. R. Kindt, G. D. Talley, S. M. Meyn, R. F. Hoyt, Jr., S. M. Marcovina, J. J. Albers, et al. 1995. Overexpression of human lecithin cholesterol acyltransferase leads to hyperalphalipoproteinemia in transgenic mice. *J. Biol. Chem.* **270**: 12269–12275.
  32. Lambert, G., N. Sakai, B. L. Vaisman, E. B. Neufeld, and B. Marteyn. 2001. Analysis of glomerulosclerosis and atherosclerosis in lecithin cholesterol acyltransferase-deficient mice. *J. Biol. Chem.* **276**: 15090–15098.
  33. Miettinen, H. E., H. Rayburn, and M. Krieger. 2001. Abnormal lipoprotein metabolism and reversible female infertility in HDL receptor (SR-BI)-deficient mice. *J. Clin. Invest.* **108**: 1717–1722.
  34. Maugeais, C., U. J. Tietge, K. Tsukamoto, J. M. Glick, and D. J. Rader. 2000. Hepatic apolipoprotein E expression promotes very low density lipoprotein-apolipoprotein B production in vivo in mice. *J. Lipid Res.* **41**: 1673–1679.
  35. Mweva, S., J. L. Paul, M. Cambillau, D. Goudouneche, P. Beaune, A. Simon, and N. Fournier. 2006. Comparison of different cellular models measuring in vitro the whole human serum cholesterol efflux capacity. *Eur. J. Clin. Invest.* **36**: 552–559.
  36. de la Llera-Moya, M., D. Drazul-Schrader, B. F. Asztalos, M. Cuchel, D. J. Rader, and G. H. Rothblat. 2010. The ability to promote efflux via ABCA1 determines the capacity of serum specimens with similar high-density lipoprotein cholesterol to remove cholesterol from macrophages. *Arterioscler. Thromb. Vasc. Biol.* **30**: 796–801.
  37. Kempen, H. J., M. Gomaschi, S. E. Bellibas, S. Plassmann, B. Zerler, H. L. Collins, S. J. Adelman, L. Calabresi, and P. L. Wijngaard. 2013. Effect of repeated apoA-IMilano/POPC infusion on lipids, (apo)lipoproteins, and serum cholesterol efflux capacity in cynomolgus monkeys. *J. Lipid Res.* **54**: 2341–2353.
  38. Alexander, E. T., C. Vedhachalam, S. Sankaranarayanan, M. de la Llera-Moya, G. H. Rothblat, D. J. Rader, and M. C. Phillips. 2011. Influence of apolipoprotein A-I domain structure on macrophage reverse cholesterol transport in mice. *Arterioscler. Thromb. Vasc. Biol.* **31**: 320–327.
  39. Matic, G. B., G. Rothe, and G. Schmitz. 2001. Flow cytometric analysis of reticulated platelets. *Curr. Protoc. Cytom.* **17**: 7.10.1–7.10.6.
  40. Dole, V. S., J. Matuskova, E. Vasile, A. Elyilalay, W. Bergmeier, M. Bernimoulin, D. D. Wagner, and M. Krieger. 2008. Thrombocytopenia and platelet abnormalities in high-density lipoprotein receptor-deficient mice. *Arterioscler. Thromb. Vasc. Biol.* **28**: 1111–1116.
  41. Basso, F., M. J. Amar, E. M. Wagner, B. Vaisman, B. Paigen, S. Santamarina-Fojo, and A. T. Remaley. 2006. Enhanced ABCG1 expression increases atherosclerosis in LDLr-KO mice on a western diet. *Biochem. Biophys. Res. Commun.* **351**: 398–404.
  42. Schneider, C. A., W. S. Rasband, and K. W. Eliceiri. 2012. NIH Image to ImageJ: 25 years of image analysis. *Nat. Methods.* **9**: 671–675.
  43. Kruth, H. S., and D. L. Fry. 1984. Histochemical detection and differentiation of free and esterified cholesterol in swine atherosclerosis using filipin. *Exp. Mol. Pathol.* **40**: 288–294.
  44. Carr, T. P., R. L. Hamilton, Jr., and L. L. Rudel. 1995. ACAT inhibitors decrease secretion of cholesteryl esters and apolipoprotein B by perfused livers of African green monkeys. *J. Lipid Res.* **36**: 25–36.
  45. Joyce, C., K. Skinner, R. A. Anderson, and L. L. Rudel. 1999. Acyl-coenzyme A:cholesteryl acyltransferase 2. *Curr. Opin. Lipidol.* **10**: 89–95.
  46. Temel, R. E., L. Hou, L. L. Rudel, and G. S. Shelness. 2007. ACAT2 stimulates cholesteryl ester secretion in apoB-containing lipoproteins. *J. Lipid Res.* **48**: 1618–1627.
  47. Rigotti, A., B. L. Trigatti, M. Penman, H. Rayburn, J. Herz, and M. Krieger. 1997. A targeted mutation in the murine gene encoding the high density lipoprotein (HDL) receptor scavenger receptor class B type I reveals its key role in HDL metabolism. *Proc. Natl. Acad. Sci. USA.* **94**: 12610–12615.
  48. Jonas, A. 1998. Regulation of lecithin cholesterol acyltransferase activity. *Prog. Lipid Res.* **37**: 209–234.
  49. Forte, T. M., G. Subbanagounder, J. A. Berliner, P. J. Blanche, A. O. Clermont, Z. Jia, M. N. Oda, R. M. Krauss, and J. K. Bielicki. 2002. Altered activities of anti-atherogenic enzymes LCAT, paraoxonase, and platelet-activating factor acetylhydrolase in atherosclerosis-susceptible mice. *J. Lipid Res.* **43**: 477–485.
  50. Jian, B., M. de la Llera-Moya, Y. Ji, N. Wang, M. C. Phillips, J. B. Swaney, A. R. Tall, and G. H. Rothblat. 1998. Scavenger receptor class B type I as a mediator of cellular cholesterol efflux to lipoproteins and phospholipid acceptors. *J. Biol. Chem.* **273**: 5599–5606.
  51. Robinet, P., Z. Wang, S. L. Hazen, and J. D. Smith. 2010. A simple and sensitive enzymatic method for cholesterol quantification in macrophages and foam cells. *J. Lipid Res.* **51**: 3364–3369.
  52. Covey, S. D., M. Krieger, W. Wang, M. Penman, and B. L. Trigatti. 2003. Scavenger receptor class B type I-mediated protection against atherosclerosis in LDL receptor-negative mice involves its expression in bone marrow-derived cells. *Arterioscler. Thromb. Vasc. Biol.* **23**: 1589–1594.

53. Duewell, P., H. Kono, K. J. Rayner, C. M. Sirois, G. Vladimer, F. G. Bauernfeind, G. S. Abela, L. Franchi, G. Nunez, M. Schnurr, et al. 2010. NLRP3 inflammasomes are required for atherogenesis and activated by cholesterol crystals. *Nature*. **464**: 1357–1361.
54. Rajamäki, K., J. Lappalainen, K. Öörni, E. Välimäki, S. Matikainen, P. T. Kovanen, and K. K. Eklund. 2010. Cholesterol crystals activate the NLRP3 inflammasome in human macrophages: a novel link between cholesterol metabolism and inflammation. *PLoS ONE*. **5**: e11765.
55. Korporaal, S. J. A., I. Meurs, A. D. Hauer, R. B. Hildebrand, M. Hoekstra, H. T. Cate, D. Praticò, J-W. N. Akkerman, T. J. C. Van Berkel, J. Kuiper, et al. 2011. Deletion of the high-density lipoprotein receptor scavenger receptor bi in mice modulates thrombosis susceptibility and indirectly affects platelet function by elevation of plasma free cholesterol. *Arterioscler. Thromb. Vasc. Biol.* **31**: 34–42.
56. Trigatti, B., S. Covey, and A. Rizvi. 2004. Scavenger receptor class B type I in high-density lipoprotein metabolism, atherosclerosis and heart disease: lessons from gene-targeted mice. *Biochem. Soc. Trans.* **32**: 116–120.
57. VanderLaan, P. A., C. A. Reardon, R. A. Thisted, and G. S. Getz. 2009. VLDL best predicts aortic root atherosclerosis in LDL receptor deficient mice. *J. Lipid Res.* **50**: 376–385.
58. Carmena, R., P. Duriez, and J-C. Fruchart. 2004. Atherogenic lipoprotein particles in atherosclerosis. *Circulation*. **109**: III-2–III-7.
59. Barter, P. J., S. Nicholls, K-A. Rye, G. M. Anantharamaiah, M. Navab, and A. M. Fogelman. 2004. Antiinflammatory properties of HDL. *Circ. Res.* **95**: 764–772.
60. Lewis, G. F., and D. J. Rader. 2005. New insights into the regulation of HDL metabolism and reverse cholesterol transport. *Circ. Res.* **96**: 1221–1232.
61. Feng, H., and X. A. Li. 2009. Dysfunctional high-density lipoprotein. *Curr. Opin. Endocrinol. Diabetes Obes.* **16**: 156–162.
62. Hewing, B., K. J. Moore, and E. A. Fisher. 2012. HDL and cardiovascular risk. *Circ. Res.* **111**: 1117–1120.
63. Otook-Kmicik, A., D. P. Mikhailidis, S. J. Nicholls, M. Davidson, J. Rysz, and M. Banach. 2012. Dysfunctional HDL: a novel important diagnostic and therapeutic target in cardiovascular disease? *Prog. Lipid Res.* **51**: 314–324.
64. Smith, J. D. 2010. Dysfunctional HDL as a diagnostic and therapeutic target. *Arterioscler. Thromb. Vasc. Biol.* **30**: 151–155.
65. Barter, P. J., and K. A. Rye. 2012. Cholesteryl ester transfer protein inhibition as a strategy to reduce cardiovascular risk. *J. Lipid Res.* **53**: 1755–1766.
66. Boden, W. E., J. L. Probstfield, T. Anderson, B. R. Chaitman, P. Desvignes-Nickens, K. Koprowicz, R. McBride, K. Teo, and W. Weintraub; AIM-HIGH Investigators. 2011. Niacin in patients with low HDL cholesterol levels receiving intensive statin therapy. *N. Engl. J. Med.* **365**: 2255–2267.
67. Hopewell, J. C., A. Offer, S. Parish, R. Haynes, J. Li, L. Jiang, M. Lathrop, J. Armitage, R. Collins, and H-T. C. Group. 2012. Environmental and genetic risk factors for myopathy in Chinese participants from HPS2-THRIVE. *Eur. Heart J.* **33**: 445.
68. Khera, A. V., M. Cuchel, M. de la Llera-Moya, A. Rodrigues, M. F. Burke, K. Jafri, B. C. French, J. A. Phillips, M. L. Mucksavage, R. L. Wilensky, et al. 2011. Cholesterol efflux capacity, high-density lipoprotein function, and atherosclerosis. *N. Engl. J. Med.* **364**: 127–135.
69. Yesilaltay, A., M. G. Morales, L. Amigo, S. Zanlungo, A. Rigotti, S. L. Karackattu, M. H. Donahee, K. F. Kozarsky, and M. Krieger. 2006. Effects of hepatic expression of the high-density lipoprotein receptor SR-BI on lipoprotein metabolism and female fertility. *Endocrinology*. **147**: 1577–1588.
70. Francone, O. L., M. Haghpassand, J. A. Bennett, L. Royer, and J. McNeish. 1997. Expression of human lecithin:cholesterol acyltransferase in transgenic mice: effects on cholesterol efflux, esterification, and transport. *J. Lipid Res.* **38**: 813–822.
71. Huszar, D., M. L. Varban, F. Rinninger, R. Feeley, T. Arai, V. Fairchild-Huntress, M. J. Donovan, and A. R. Tall. 2000. Increased LDL cholesterol and atherosclerosis in LDL receptor-deficient mice with attenuated expression of scavenger receptor B1. *Arterioscler. Thromb. Vasc. Biol.* **20**: 1068–1073.
72. Ji, Y., B. Jian, N. Wang, Y. Sun, M. L. Moya, M. C. Phillips, G. H. Rothblat, J. B. Swaney, and A. R. Tall. 1997. Scavenger receptor BI promotes high density lipoprotein-mediated cellular cholesterol efflux. *J. Biol. Chem.* **272**: 20982–20985.
73. Tabas, I., S. Marathe, G. A. Keesler, N. Beatini, and Y. Shiratori. 1996. Evidence that the initial up-regulation of phosphatidylcholine biosynthesis in free cholesterol-loaded macrophages is an adaptive response that prevents cholesterol-induced cellular necrosis. Proposed role of an eventual failure of this response in foam cell necrosis in advanced atherosclerosis. *J. Biol. Chem.* **271**: 22773–22781.
74. Fazio, S., A. S. Major, L. L. Swift, L. A. Gleaves, M. Accad, M. F. Linton, and R. V. Farese. 2001. Increased atherosclerosis in LDL receptor-null mice lacking ACAT1 in macrophages. *J. Clin. Invest.* **107**: 163–171.
75. Nofer, J. R., M. F. Brodde, and B. E. Kehrel. 2010. High-density lipoproteins, platelets and the pathogenesis of atherosclerosis. *Clin. Exp. Pharmacol. Physiol.* **37**: 726–735.
76. Nofer, J. R., G. Herminghaus, M. Brodde, E. Morgenstern, S. Rust, T. Engel, U. Seedorf, G. Assmann, H. Bluethmann, and B. E. Kehrel. 2004. Impaired platelet activation in familial high density lipoprotein deficiency (Tangier disease). *J. Biol. Chem.* **279**: 34032–34037.
77. Hansson, G. K., and P. Libby. 2006. The immune response in atherosclerosis: a double-edged sword. *Nat. Rev. Immunol.* **6**: 508–519.
78. Föger, B., M. Chase, M. J. Amar, B. L. Vaisman, R. D. Shamburek, B. Paigen, J. Fruchart-Najib, J. A. Paiz, C. A. Koch, R. F. Hoyt, et al. 1999. Cholesteryl ester transfer protein corrects dysfunctional high density lipoproteins and reduces aortic atherosclerosis in lecithin cholesterol acyltransferase transgenic mice. *J. Biol. Chem.* **274**: 36912–36920.
79. El Bouhassani, M., S. Gilbert, M. Moreau, F. Saint-Charles, M. Treguier, F. Poti, M. J. Chapman, W. Le Goff, P. Lesnik, and T. Huby. 2011. Cholesteryl ester transfer protein expression partially attenuates the adverse effects of SR-BI receptor deficiency on cholesterol metabolism and atherosclerosis. *J. Biol. Chem.* **286**: 17227–17238.
80. Bérard, A. M., B. Föger, A. Remaley, R. Shamburek, B. L. Vaisman, G. Talley, B. Paigen, R. F. Hoyt, Jr., S. Marcovina, H. B. Brewer, Jr., et al. 1997. High plasma HDL concentrations associated with enhanced atherosclerosis in transgenic mice overexpressing lecithin-cholesteryl acyltransferase. *Nat. Med.* **3**: 744–749.
81. Mehlum, A., M. Muri, T. A. Hagve, L. A. Solberg, and H. Prydz. 1997. Mice overexpressing human lecithin: cholesterol acyltransferase are not protected against diet-induced atherosclerosis. *APMIS*. **105**: 861–868.
82. Hoeg, J. M., S. Santamarina-Fojo, A. M. Bérard, J. F. Cornhill, E. E. Herderick, S. H. Feldman, C. C. Haudenschild, B. L. Vaisman, R. F. Hoyt, S. J. Demosky, et al. 1996. Overexpression of lecithin:cholesterol acyltransferase in transgenic rabbits prevents diet-induced atherosclerosis. *Proc. Natl. Acad. Sci. USA*. **93**: 11448–11453.